Prognostics and Structural Health Assessment Using Uncertain Measured Response Information

Achintya Haldar and Abdullah Al-Hussein

Abstract The authors and their team members have been working on developing implementable techniques for the objective rapid assessment of structural health (RASH) just after major natural and man-made events or in the context of maintenance over a period of time. They used the system-identification techniques by eliminating some of its weaknesses. For easier implementation, the excitation information was completely ignored. To locate defects and their severity at the local element level, the structures were represented by finite elements. By tracking the changes in the stiffness parameters of each element, the location(s) and severity of defects are assessed. The team conducted extensive analytical and laboratory investigations to verify all the methods. They had to overcome several challenges related to the conceptual and analytical development, data processing, and the presence of uncertainty in the every phase. To consider nonlinearity in the system identification process, a method known as Generalized Iterative Least Squares-Extended Kalman Filter-Unknown Input (GLIS-EKF-UI), was developed earlier. Since it failed to identify structures in some cases, the authors recently proposed a new method denoted as Unscented Kalman Filter—Unknown Input-Weighted Global Iterations (UKF-UI-WGI). With the help of informative examples, the superiority of UKF-UI-WGI over GLIS-EKF-UI is documented in this paper. Since at the beginning of an inspection, the defects and their severity are expected to be unknown, the authors recommend UKF-UI-WGI for the rapid assessment of health of infrastructures.

Keywords Structural health assessment · Uncertain measured information · Kalman filters · Nonlinear system identification · Unknown input excitation

A. Haldar (✉) · A. Al-Hussein
University of Arizona, 1209 E. 2nd St, Tucson, AZ 85721, USA
e-mail: haldar@u.arizona.edu

A. Al-Hussein
e-mail: abdullaa@email.arizona.edu

U. Kumar et al. (eds.), *Current Trends in Reliability, Availability, Maintainability and Safety*, Lecture Notes in Mechanical Engineering,
DOI 10.1007/978-3-319-23597-4_13

1 Introduction

ICRESH-ARMS 2015 provides a unique opportunity to discuss all the issues related to Prognostic and Structural Health Assessment. In fact, the first two issues of Life Cycle Reliability and Safety Engineering published by the Society for Reliability and Safety (SRESA) in 2015 are dedicated to the related topics. The related areas have become one of the most active research topics and have attracted multi-disciplinary interest. Extending life of infrastructures instead of replacing them has become a major challenge to engineers [9]. Structural health assessment just after a natural event or a man-made event has also become a part of inspection protocol. Non-destructive evaluation or inspection techniques of various degrees of sophistication are developed to help the assessment process. Smart sensing technologies, high quality data acquisition systems, mitigation techniques for noise contamination, digital communications, sophisticated computational techniques, etc., have been developed. This general area is commonly known as structural health assessment (SHA) or structural health monitoring (SHM).

Any automated monitoring practice that seeks to assess the health of a structure can be considered as SHM [7]. It implies that the health of a structure can be monitored in an automated manner by tracking the initiation or growth of a defect already present in the system. Since visual inspections may not be adequate for this purpose, sensors and the interpretation of their readings are essential for SHM. In spite of its recent impressive developments, it is not generally used in real world applications. Continuous accurate measurements of any output is a major challenge considering power sources necessary for operation, data transfer and storage, failure or sensors getting out of calibration, etc. The users generally assume that the technology is not fully developed for practical applications.

Objective rapid assessment of structural health (RASH) is essential just after a visual inspection or after a major natural event like strong earthquake or high wind or man-made event like blast or explosion, or in the context of maintenance. There is a potential for significant loss of economic activities in a region without such assessment. There are significant developments in the related areas. These areas are the subject of this paper.

2 Rapid Assessment of Structural Health

All defects are not equally important in maintaining the overall structural health. Thus, some of the major objectives of RASH are to locate defects at the local element level, assess their severity, and take remedial actions when necessary. If defects are repaired, it is important to know if they are repaired properly and all major defects are identified. To achieve these objectives, the process of listening to audible variations of responses due to tapping of structural surface has been used

over centuries. Visual inspections at regular intervals are also suggested in many design codes. They can be broadly categorised as non-model based non-destructive inspection (NDI) techniques. If location of a defect is known, the profession now have technological sophistication to inspect it using instrument-based Penetrate Testing, Magnetic Particle Testing, Radiographic Testing, Ultrasonic Testing, Eddy Current Testing, Acoustic Emission Testing, Thermal Infrared Testing, etc.

For most large civil infrastructures, the location, number, and severity of defects may not be known in advanced. Sometimes, defects may be hidden behind obstructions like fire-proofing materials. Thus, instrument-based non-model approaches may not satisfied our needs. In the recent past, a consensus started developing about the use of measured time domain dynamic responses at the global level to assess the current structural health at the local element level. By appropriately tracking the signature embedded in the measurements, the structural health can be assessed.

The research team at the University of Arizona has been working on developing testing protocols for RASH for over two decades. After conducting extensive literature review, the team concluded that to locate defects, number, and their severity, it will be helpful if structures are represented by finite elements and their dynamic responses are measured in time domain representing their current state. By comparing the identified dynamic properties, essentially the stiffness properties of the elements, with the expected values, or reference values obtained from the design drawings, or changes from the previous values if inspections are carried out periodically, or variations from one member to another with similar sectional properties, the location(s), number, and severity of defects can be established at the element level. The concept is based on the axiom that the presence of defects will alter the dynamic responses and by tracking the signature embedded in the responses, the structural health can be assessed rapidly.

3 System Identification-Based Rash

By measuring dynamic excitation and response information, the stiffness parameter of all the elements in the finite element representation can be evaluated using an inverse mathematical concept commonly known as the system identification (SI) technique. However, Maybeck [21] correctly pointed out that deterministic mathematical models and control theories do not appropriately represent the behavior of a physical system and thus the SI-based method may not be appropriate. The research team successfully demonstrated that SI-based concept can be used for RASH if the different sources of uncertainty are accounted for appropriately and the system parameters are evaluated in an optimal sense using proper data processing algorithm.

3.1 System Identification with Unknown Input

One of the basic requirements for RASH is the simplicity in the inspection process. It is known to the profession that measuring dynamic excitation forces in the field condition can be very error prone due to inherent noises in the sensors and contamination due to multiple sources of excitation which is beyond the control of the inspector. It will be very desirable if a system can be identified using only measured response information completely ignoring the excitation information. The team developed several such techniques, commonly known as Iterative Least Squares with Unknown Input (ILS-UI) [24], Modified ILS-UI or MILS-UI [19], and Generalized ILS-UI or GILS-UI [18]. Mathematical concepts used to develop them cannot be discussed here due to lack of space but widely available in the literature. One major advantage of these procedures is that they are not very sensitive to the noises present in the response time histories.

3.2 System Identification with Unknown Input and Limited Response Information—Kalman Filter

One major deficiency of the methods discussed in the previous section is that they require response time histories at all DDOFs. To assess health of real infrastructures, it may be practically impossible and very expensive to install sensors at all DDOFs. In most cases, only a small part of the structure can be instrumented. When available responses are limited, generally Kalman filter (KF)-based concept is used. Kalman filter [15, 16] is a set of mathematical equations that provides efficient computational means in a recursive manner to estimate the state of a process, in a way that minimizes the mean of squared error, and calculates the best estimate of states from the noisy sensor responses [12, 26]. It is a time domain filter and is very powerful in several aspects. One of its limitations is that it is applicable for linear systems. If KF is used for RASH, the identification process becomes nonlinear. This is due to the fact that the identification of the unknown parameters jointly with dynamic responses is a nonlinear identification problem even if the structural system is linear. For nonlinear SI, extended Kalman filter (EKF) will be an attractive choice. It extends the linear Kalman filter to handle nonlinear systems based on a first-order linearization of the nonlinear statistical distributions of the variables. For RASH, EKF is an important requirement.

To implement EKF for RASH, the excitation force and the initial state vector must be known. The first requirement will defeat the purpose of SHA without input or ILS-UI. The second requirement is the final product of any inspection strategy and will not be available at the initiation of the inspection process. These two implementation requirements essentially limit the use of the basic KF concept for RASH.

Since EKF is very powerful, the team [25] decided to generate the required information to implement it. Suppose only a small part of the structure is instrumented. For the ease of discussion, it will be denoted as substructure. It is assumed that the responses at all DDOFs of the substructure will be measured. Then, the ILS-UI concept can be used to identify the stiffness parameter of all the elements in the substructure. All the beams and columns in the whole structure are expected to have similar cross sectional properties. Assuming the substructure contains a beam and a column element, all the elements in the whole structure can be assigned respective properties and the initial state vector of the structure will now be available. One very attractive attribute of ILS-UI is that it identifies the unknown excitation time history. Thus, with the introduction of the substructure concept, the two implementation requirements of EKF can be satisfied and the health of large real structural systems can be assessed using limited noise-contaminated responses without using any information on excitation.

The concept just discussed is known as Generalized Iterative Least Squares—Extended Kalman Filter—Unknown Input or GILS-EKF-UI. It can be implemented in two stages. In Stage 1, based on the available response information, a substructure can be identified. Using ILS-UI on the substructure, the unknown excitation time history and the stiffness parameter of all the elements in the substructure can be identified. The information will help to develop the initial state vector for the whole structure. Then in Stage 2, the EKF concept will be used to identify the stiffness parameter of all the elements in the structure. In this way, the number, location, and severity of defects can be assessed very accurately. The mathematical theories behind the two stages are discussed very briefly below.

4 Mathematics of Gils-Ekf-Ui

4.1 Stage 1—ILS-UI

The governing differential equation of motion using Rayleigh damping for the substructure can be expressed as:

$$\mathbf{M}_{sub}\ddot{\mathbf{X}}_{sub}(t) + (\alpha\mathbf{M}_{sub} + \beta\mathbf{K}_{sub})\dot{\mathbf{X}}_{sub}(t) + \mathbf{K}_{sub}\mathbf{X}_{sub}(t) = \mathbf{f}_{sub}(t) \tag{1}$$

where $\mathbf{M}_{sub}$ is the global mass matrix, generally considered to be known; $\mathbf{K}_{sub}$ is the global stiffness matrix; $\ddot{\mathbf{X}}_{sub}(t)$, $\dot{\mathbf{X}}_{sub}(t)$, and $\mathbf{X}_{sub}(t)$ are the vectors containing the acceleration, velocity, and displacement, respectively, at time t; $\mathbf{f}_{sub}(t)$ is the input excitation vector at time t; and α and β are the mass and stiffness proportional Rayleigh damping coefficients, respectively. The subscript 'sub' is used to denote substructure.

The global mass and stiffness matrix can be formulated using standard procedure. The stiffness parameter for the ith element, k_i is defined as E_iI_i/L_i, where $L_{i,}$ I_i and E_i are the length, moment of inertia, and modulus of elasticity, respectively. The **P** vector contains all the unknown parameters and can be defined as:

$$\mathbf{P} = [k_1 \; k_2 \; \cdots \; k_{nesub} \; \beta k_1 \; \beta k_2 \; \cdots \; \beta k_{nesub} \; \alpha]^T \tag{2}$$

Using the least squares concept, it can be estimated as [24]:

$$\mathbf{P} = \left(\mathbf{A}^T\mathbf{A}\right)^{-1}\mathbf{A}^T\mathbf{F} \tag{3}$$

where **A** matrix contains the measured displacement and velocity responses at time point t; **F** vector contains the unknown input excitations and the inertia forces at time point t; and the responses are measured at equal interval of Δt for q time points. Since the input excitation $\mathbf{f}_{sub}$ is unknown, the force vector **F** in Eq. (3) is partially known and the iteration process cannot be initiated. To start the iteration process, the excitation information can be initially assumed to be zero for all the time points as discussed in [18]. The iteration process is continued until the excitation time history converges at all time points, considering two successive iterations, with a predetermined tolerance level. A tolerance level is set to be 10^{-8} in this study.

It is important to note that only acceleration time histories will be measured during an inspection. However, velocity and displacement time histories are necessary to implement the concept. The acceleration time histories can be successively integrated to generate the velocity and displacement time histories as discussed in more details in [8, 10, 22].

4.2 Stage 2—Implementation of EKF Concept

To implement the EKF concept, the differential equation in state-space form and the discrete time measurements can be expressed as:

$$\dot{\mathbf{Z}}(t) = f[\mathbf{Z}(t), t] \tag{4}$$

$$\mathbf{Y}(k) = h\,[\mathbf{Z}(k), t] + \mathbf{V}(k) \tag{5}$$

where $\mathbf{Z}(t)$ is the state vector at time t; $\dot{\mathbf{Z}}(t)$ is the time derivative of the state vector; f is a nonlinear function of the state; $\mathbf{Y}(k)$ is the measurement vector; h is the function that relates the state to the measurement; $\mathbf{V}(k)$ is a zero-mean, uncorrelated, white noise process with variance $R(k)$, and represented by $E[V(k)\; V^T(j)] = R(k)\delta(k-j)$, where $\delta(k-j)$ is the Kronecker delta function; that is $\delta(k-j) = 1$ if $k = j$, and $\delta(k-j) = 0$ if $k \neq j$.

For a structure represented by N number of degrees of freedom and L number of elements, the vectors $\mathbf{Z}(t)$ and $\dot{\mathbf{Z}}(t)$ are of size $(2\,N + L) \times 1$, L is the total number of unknown stiffness parameters. They are formed in the following way:

$$\mathbf{Z}(t) = \begin{bmatrix} \mathbf{Z}_1(t) \\ \mathbf{Z}_2(t) \\ \mathbf{Z}_3(t) \end{bmatrix} = \begin{bmatrix} \mathbf{X}(t) \\ \dot{\mathbf{X}}(t) \\ \tilde{\mathbf{K}} \end{bmatrix} \tag{6}$$

$$\dot{\mathbf{Z}}(t) = \begin{bmatrix} \dot{\mathbf{X}}(t) \\ \ddot{\mathbf{X}}(t) \\ 0 \end{bmatrix} = \begin{bmatrix} \dot{\mathbf{X}}(t) \\ -\mathbf{M}^{-1}[\mathbf{K}\mathbf{X}(t) + (\alpha\mathbf{M} + \beta\mathbf{K})\dot{\mathbf{X}}(t) - \mathbf{f}(t)] \\ 0 \end{bmatrix} \tag{7}$$

where $\tilde{\mathbf{K}} = [\,k_1 \quad k_2 \quad \cdots \quad k_{ne}\,]^T$ is column vector of size $(L \times 1)$.

For the identification of the whole structure, acceleration responses will be measured at a fewer (B) number of DDOFs. The accelerations will be integrated twice to obtain the velocities and displacements, as described in [22]. The vector $\mathbf{Y}(k)$ will have size $(2B \times 1)$ and will contain information on observed displacements and velocities.

Therefore, the discrete time measurement model is linear and it can be expressed at any discrete time k as:

$$\mathbf{Y}(k) = \mathbf{H} \cdot \mathbf{Z}(k) + \mathbf{V}(k) \tag{8}$$

where matrix $\mathbf{H}$ is the measurement matrix of size $2B \times (2\,N + L)$.

The filtering process in EKF can be started after initialization of state vector $\mathbf{Z}(0|0)$, which can be assumed to be Gaussian random variable with state mean $\hat{\mathbf{Z}}(0|0)$ and error covariance of $\mathbf{P}(0|0)$ i.e., $\mathbf{Z}(0|0) \sim N[\hat{\mathbf{Z}}(0), \mathbf{P}(0)]$.

The initial error covariance matrix $\mathbf{P}(0|0)$ contains information on the errors in the observed displacement and velocity responses, and in the initial values assigned to the unknown stiffness parameters of the whole structure. It is generally assumed to be diagonal and can be expressed as:

$$\mathbf{P}(0|0) = \begin{bmatrix} \mathbf{P}_x(0|0) & 0 \\ 0 & \mathbf{P}_s(0|0) \end{bmatrix} \tag{9}$$

where $\mathbf{P}_x(0|0)$ is a $(2\,N \times 2\,N)$ diagonal matrix, contains initial error covariance for observed responses; $\mathbf{P}_s(0|0)$ is a $(L \times L)$ diagonal matrix, contains initial error covariance for matrix $\tilde{\mathbf{K}}$. In the present study, a value of 1.0 is considered for the diagonal entries of $\mathbf{P}_x(0|0)$. Jazwinski [12] and Al-Hussein and Haldar [2, 4] pointed out that the diagonal entries for $\mathbf{P}_s(0|0)$ should be large positive numbers to accelerate the convergence of the local iteration process. A value of 1000 is used in this study.

The basic filtering process in EKF is the same Kalman filter (KF), i.e. propagation of the state mean and covariance from time k to one step forward in time

k + 1, and then updating them when the measurement at time k + 1 becomes available. Mathematically the steps can be expressed as:

(i) Prediction of state mean $\hat{\mathbf{Z}}(k+1|k)$ and its error covariance matrix $\hat{\mathbf{P}}(k+1|k)$ for the next time increment k + 1 as:

$$\hat{\mathbf{Z}}(k+1|k) = \hat{\mathbf{Z}}(k|k) + \int_{k\Delta t}^{(k+1)\Delta t} \dot{\hat{\mathbf{Z}}}(t|k)dt \tag{10}$$

$$\mathbf{P}(k+1|k) = \mathbf{\Phi}(k+1|k)\mathbf{P}(k|k)\mathbf{\Phi}^T(k+1|k) \tag{11}$$

(ii) Using measurement $\mathbf{Y}(k+1)$ and Kalman gain $\mathbf{K}(k+1)$ available at time k + 1, updated state mean $\hat{\mathbf{Z}}(k+1|k+1)$ and error covariance matrix $\hat{\mathbf{P}}(k+1|k+1)$ can be obtained as:

$$\hat{\mathbf{Z}}(k+1|k+1) = \hat{\mathbf{Z}}(k+1|k) + \mathbf{K}(k+1)[\mathbf{Y}(k+1) - \mathbf{H} \cdot \hat{\mathbf{Z}}(k+1|k)] \tag{12}$$

$$\begin{aligned}\mathbf{P}(k+1|k+1) = {} & [\mathbf{I} - \mathbf{K}(k+1)\ \mathbf{H}]\ \mathbf{P}(k+1|k)\ [\mathbf{I} - \mathbf{K}(k+1)\ \mathbf{H}]^T \\ & + \mathbf{K}(k+1)\ \mathbf{R}(k+1)\ \mathbf{K}^T(k+1)\end{aligned} \tag{13}$$

where

$$\mathbf{K}(k+1) = \mathbf{P}(k+1|k)\mathbf{H}^T[\mathbf{H}\mathbf{P}(k+1|k)\mathbf{H}^T + \mathbf{R}(k+1)]^{-1} \tag{14}$$

where, $\mathbf{\Phi}(k+1|k)$ is the state transfer matrix from time k to k + 1; $\mathbf{K}(k+1)$ and $\mathbf{R}(k$ + 1) is the Kalman gain matrix and diagonal noise covariance matrix, respectively, at time k + 1. Detail procedure for calculation of $\mathbf{\Phi}$, $\mathbf{K}$, and $\mathbf{M}$ can be found in [17]. The symbol · stands for matrix multiplication. In the present study, diagonal entries in the noise covariance matrix $\mathbf{R}(k)$ are considered to be 10^{-4}.

5 UKF Based SI Concept

As will be discussed later, GILS-EKF-UI was successfully verified by conducting extensive analytical and laboratory investigations. In the laboratory investigations, the transverse acceleration time-histories were measured by capacitance accelerometers and angular rotation by autocollimators [20, 23]. To avoid contamination by other sources of excitations beyond the control of the inspector, responses were collected at a high sampling rate, 4000 cycles per second, for a fraction of a second. More recently it was observed that GILS-EKF-UI failed to converge or identify a structure when the sampling rate is much lower than what

was used for the laboratory investigation. Upon further investigations, the authors concluded that the major reason for the non-convergence is the presence of higher level of nonlinearity. GILS-EKF-UI is supposed to identify a system in the presence of some degree of nonlinearity but the threshold is not known at this time. The first-order linearity used in EKF may not be sufficient to address more severe level of nonlinearities in the responses.

The authors [1] concluded that the unscented Kalman filter (UKF) concept can be used for highly nonlinear system identification problems. The UKF concept was developed by Julier et al. [14] to address the shortcoming of EKF. The UKF concept was developed based on unscented transformation (UT) with the underlying assumption that approximating a Gaussian distribution is easier than approximating a nonlinear transformation. UKF uses deterministic sampling to approximate the state distribution as a Gaussian Random Variable. The sigma points are chosen to capture the true mean and covariance of state distribution. They are propagated through the nonlinear system. UKF determines the mean and covariance accurately to the second order, while the EKF is only able to obtain first order accuracy [13].

The main difference between the EKF and UKF procedures is in the prediction step, i.e. prediction of the state vector and its error covariance using mathematical model of the system. They are the same in the updating step. In the prediction step of EKF, Jacobian matrices are used to linearize the nonlinear equations so that the linear KF can be used. However, in the prediction step of UKF, a number of state vectors or so-called sigma points is generated and then propagated through the nonlinear equations to get more accurate estimate. Thus, to implement the UKF procedure, instead of using Eqs. (10) and (11) of the EKF procedure, the following equations are necessary.

5.1 Sigma Points Calculation Step

At the current state vector $\hat{\mathbf{Z}}(k|k)$, sets of $2n + 1$ symmetric sigma points are generated so that they have the same mean and covariance of $\hat{\mathbf{Z}}(k|k)$ as following:

$$\begin{aligned} \boldsymbol{\chi}_0(k|k) &= \hat{\mathbf{Z}}(k|k) \\ \boldsymbol{\chi}_i(k|k) &= \hat{\mathbf{Z}}(k|k) + \sqrt{(\lambda+n)}\mathbf{C}_{col,i} \quad i = 1,\ldots,n \\ \boldsymbol{\chi}_{i+n}(k|k) &= \hat{\mathbf{Z}}(k|k) - \sqrt{(\lambda+n)}\mathbf{C}_{col,i} \quad i = 1,\ldots,n \end{aligned} \tag{15}$$

where

$$\lambda = \varphi^2(n+\gamma) - n \tag{16}$$

in which $\mathbf{C}$ is a square root of the covariance matrix such that $\mathbf{P}(k) = \mathbf{C} \cdot \mathbf{C}^T$; $\mathbf{C}_{col,i}$ is the ith column of $\mathbf{C}$'s matrix; n is the dimension of the state vector ($n = 2\,N + L$); The parameter φ determines the spread of the sigma points around the mean. Typical range value for φ is ($0 \leq \varphi \leq 1$). The parameter γ is a tertiary scaling factor and is usually set equal to 0. In fact, parameter γ can be used to reduce the higher order errors of the mean and the covariance approximations. Note that sigma points are a set of vectors whose components are real numbers.

5.2 Prediction Step

The sigma points are propagated through the nonlinear dynamic equation as:

$$\boldsymbol{\chi}_i(k+1|k) = \boldsymbol{\chi}_i(k|k) + \int_{k\Delta t}^{(k+1)\Delta t} f[\mathbf{Z}(t), t]dt \quad i = 1, \ldots, 2n \tag{17}$$

The predicted state vector $\hat{\mathbf{Z}}(k+1|k)$ can be shown to be:

$$\hat{\mathbf{Z}}(k+1|k) = \sum_{i=0}^{2n} W_i \; \boldsymbol{\chi}_i(k+1|k) \tag{18}$$

and its predicted error covariance matrix $\mathbf{P}(k+1|k)$ can be expressed as:

$$\begin{aligned}\mathbf{P}(k+1|k) = &\sum_{i=0}^{2n} W_i \left[\boldsymbol{\chi}_i(k+1|k) - \hat{\mathbf{Z}}(k+1|k)\right]\left[\boldsymbol{\chi}_i(k+1|k) - \hat{\mathbf{Z}}(k+1|k)\right]^T \\ &(1 - \varphi^2 + \psi)\left[\boldsymbol{\chi}_0(k+1|k) - \hat{\mathbf{Z}}(k+1|k)\right]\left[\boldsymbol{\chi}_0(k+1|k) - \hat{\mathbf{Z}}(k+1|k)\right]^T\end{aligned} \tag{19}$$

where ψ is the secondary scaling factor used to emphasize the weighting on the zero's sigma point for the covariance calculation. The value of ψ is greater than 0 and the best value is 2 for Gaussian distribution. The weight factor W_i can be shown to be:

$$W_0 = \frac{\lambda}{\lambda + n} \qquad i = 0 \tag{20}$$

$$W_i = \frac{1}{2(\lambda + n)} \quad i = 1, \ldots, 2n \tag{21}$$

It is important to point out here that in this study the measurement model is linear and linear KF is used to predict the measurement vector and its error covariance matrix.

5.3 Improvements in UKF Algorithm

When the EKF concept was used in the context of ILS-UI, i.e. the two-stage concept used in GILS-EKF-UI, it failed to converge in some cases. The authors observed that the use of UKF to identify large structural systems were very limited in the literature. Most of the reported works were developed to identify shear-type structures with very few DDOFs using long duration responses in one global iteration. Suppose that the responses are available for q time points. The iteration processes between successive time points in the UKF procedure are termed as local iterations and the iteration processes for all q time points are termed as a global iteration. The three steps of the UKF (sigma point, prediction and updating operations) are carried out for all q time points.

To obtain optimal, stable, and convergent solutions of the SI process, the authors proposed to use several global iterations using responses collected for a fraction of second. They noted that the error covariance matrix of the stiffness parameters reduced significantly during the successive global iterations and the identified stiffness values sometimes converge to the wrong values particularly when the initial values are far from the expected values representing defective states. This prompted the authors [3, 4] to introduce a weighted global iteration factor, w, to the error covariance matrix after the first global iteration so that the algorithm can detect the stiffness parameters with incorrect initial value but converges to the correct solution. In the second global iteration, the initial values of the stiffness parameters are the same as that of obtained at the completion of first global iteration. A weight factor w is introduced in the stiffness covariance matrix obtained at the completion of the first global iteration to amplify it and then used it as the initial stiffness covariance in the second global iteration. The weighted global iteration concept can be mathematically presented as:

$$\hat{\mathbf{Z}}^{(2)}(0|0) = \begin{bmatrix} \hat{\mathbf{X}}^{(2)}(0|0) \\ \dot{\hat{\mathbf{X}}}^{(2)}(0|0) \\ \tilde{\mathbf{K}}^{(2)}(0|0) \end{bmatrix} = \begin{bmatrix} \hat{\mathbf{X}}^{(1)}(0|0) \\ \dot{\hat{\mathbf{X}}}^{(1)}(0|0) \\ \tilde{\mathbf{K}}^{(1)}(q|q) \end{bmatrix} \tag{22}$$

$$\mathbf{P}^{(2)}(0|0) = \begin{bmatrix} \mathbf{P}_x^{(1)}(0|0) & 0 \\ 0 & w\mathbf{P}_s^{(1)}(q|q) \end{bmatrix} \tag{23}$$

The same processes of local iterations are carried out for all the time points and a new set of state vector and error covariance matrix are obtained at the completion of second global iteration. The weighted global iteration processes are continued until

the estimated error in the identified stiffness parameters at the end of two consecutive global iterations becomes smaller than a predetermined convergence criterion (ε_s).

$$\left|\tilde{\mathbf{K}}^{(i)}(q|q) - \tilde{\mathbf{K}}^{(i-1)}(q|q)\right| \leq \varepsilon_s \times \left|\tilde{\mathbf{K}}^{(i-1)}(q|q)\right| \tag{24}$$

where i represents the ith global iteration. ε_s is considered to be 1 % in this study.

Although the weighted global iterations play an important role in the later stage to assure convergence; the global iteration procedure does not guarantee the convergence of the iteration scheme. If they diverge, the best estimated values based on minimum objective function $\bar{\theta}$ are considered, as discussed in [4, 11].

The procedure developed this way will be denoted as Unscented Kalman Filter —Unknown Input- Weighted Global Iterations or UKF-UI-WGI. It will be implemented in two stages in the same way as that of GILS-EKF-UI. It will not require any additional resources but it will improve the defect detection capability in a significant way, as will be elaborated further with the help of several informative examples.

6 Examples

It is hoped that the sequential development processes used by the research team to develop several RASHs for infrastructures are informative. However, during each phase of the development, the reviewers of technical papers commented that the procedures were reasonable from the theoretical point of view but could not be used for the health assessment of real infrastructures. This prompted the research team to initiate several laboratory investigations. One of them is discussed briefly below.

6.1 Example 1

6.1.1 Description of the Frame and Dynamic Testing

A two-dimensional one-bay three-story steel frame, shown pictorially in Fig. 1, was initially tested to verify the EKF procedure [20]. To fit the testing facilities, the frame was scaled to one-third of its actual dimensions. The scaled frame has a bay width of 3.05 m and story height of 1.22 m. The frame consists of nine members; six columns and three beams. Steel section of size S4 × 7.7 was used for all the beams and columns in order to minimize the effects of fabrication defects and differences in material properties. The frame was reconfigurable, i.e. bolted joints were used so that the defect-free and defective members could be interchanged to study defect detection capability. Several types of defects, very severe to minor in

Fig. 1 The pictorial view of the frame

nature, were introduced. Some of the defect scenarios considered were removing a member completely, loss of area of a member over a finite length, multiple cracks in a member, one crack in a member, loosening bolts at joints, and multiple combinations of these defects. The same response information was used to verify both GILS-EKF-UI and UKF-UI-WGI in the following sections.

The frame consists of 9 members; 3 beams and 6 columns. The frame is represented by the finite element (FE) with 9 elements and 8 nodes. Each node has three DDOFs; two translational and one rotational. The support condition at the bases is considered to be fixed. Therefore, the total number of DDOFs for the frame is 18. The actual stiffness parameters k_i, defined in terms of $(E_i I_i / L_i)$, for the beam and column are estimated to be 96500 and 241250 N-m, respectively. The first two natural frequencies of the defect-free frame were estimated experimentally to be $f_1 = 9.76$ Hz and $f_2 = 34.12$ Hz. Then, assuming the same damping for the first two significant frequencies, a procedure suggested in [6], is used to calculate the Rayleigh damping coefficients α and β. They are found to be 1.1453681 and 0.0000871, respectively. The frame is excited by a sinusoidal load $f(t) = 1.4 \sin(58.23t)$ N applied at node 1, as shown in Fig. 2. Before conducting any test, numerous analytical verifications were carried under various testing conditions. For the analytical verifications, the responses of the frame in terms of displacement, velocity and acceleration time histories were numerically generated using a commercial software ANSYS (ver. 15.0) [5] at all 9 DDOFs (responses at nodes 1, 2 and 3) of the substructure for all cases. The frame is identified using responses from 0.02 to 0.32 s with time increment of 0.00025 s providing a total of 1201 time points. For the laboratory investigation, the translational and rotational acceleration

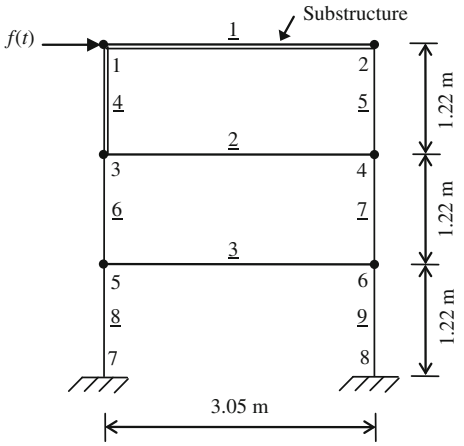

Fig. 2 Finite element representation of the test frame

Table 1 Stiffness parameter (*EI/L*) identification for the substructure—defect-free frame

Member	Nominal (N-m)	Identified	Change (%)
(1)	(2)	(3)	(4)
k_1	96500	96502	0.002
k_4	241250	241255	0.002

time histories were measured. They were successively integrated to generate velocity and displacement time histories as suggested in [8, 22].

6.1.2 Identification of the Defect-Free State of the Frame

To implement both the GILS-EKF-UI and UKF-UI-WGI methods, the substructure used is shown in double lines in Fig. 2. The stiffness parameters of the two elements in the substructure using ILS-UI in Stage 1 are identified and the results are summarized in Table 1. The results indicate that the substructure is identified very accurately. As mentioned earlier, ILS-UI also identifies the unknown excitation force. Both the actual and identified excitation time histories are shown in Fig. 3. The figure clearly indicates the unknown excitation time history is also identified very accurately.

The errors in measurement noises (*R)* in Eq. 5 are one of the important factors that influence the identification of the stiffness parameter. Two different values of *R* (10^{-3} and 10^{-4}) are considered in this study. Using the information from Stage 1, the stiffness parameter of all the nine members of the whole frame is identified using the GILS-EKF-UI and UKF-UI-WGI methods. The results are summarized in Table 2. As commonly used in the literature, the errors are defined as the percentage deviation of identified values, representing the current state, with respect to the initial theoretical values. The maximum acceptable error in the identification is

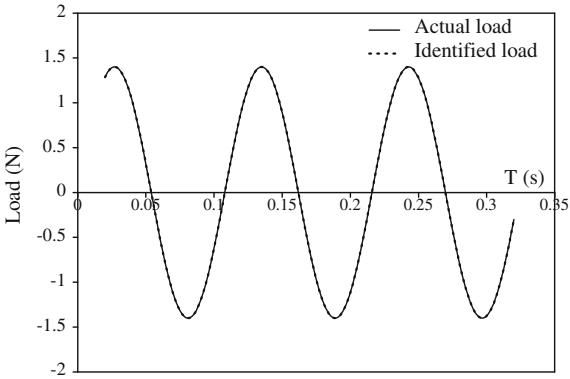

Fig. 3 Actual and identified force time histories using ILS-UI for defect-free case

Table 2 Stiffness parameter (*EI/L*) identification for defect-free frame

Member	Nominal (N-m)	Error in Identification (%)			
		$R = 10^{-4}$		$R = 10^{-3}$	
		EKF	UKF	EKF	UKF
(1)	(2)	(3)	(4)	(5)	(6)
k_1	96500	0.002	−0.069	0.000	−0.030
k_2	96500	0.062	0.091	0.064	0.054
k_3	96500	0.047	0.096	−0.102	−0.065
k_4	241250	−0.063	−0.063	−0.004	−0.007
k_5	241250	−0.237	−0.073	−0.063	−0.001
k_6	241250	−0.096	0.013	−0.003	0.009
k_7	241250	−0.338	−0.104	−0.011	−0.015
k_8	241250	−0.032	−0.222	−0.011	−0.040
k_9	241250	−0.105	−0.206	−0.016	−0.039

about 10 % reported in the literature [2]. The results in Table 2 clearly indicate that both methods identified the stiffness parameters of all the members reasonably well for both measurement errors. In an overall sense, UKF-UI-WGI identified the frame more accurately than GILS-EKF-UI. Since the differences in identified stiffness parameters are relatively small, the health of the frame can be considered as defect-free.

6.1.3 Health Assessment of Defective Frame

After successfully identifying the defect-free frame, several defective states of the frame were considered, as discussed earlier. Only two defect scenarios are presented in the following sections.

Fig. 4 Defect in member 3

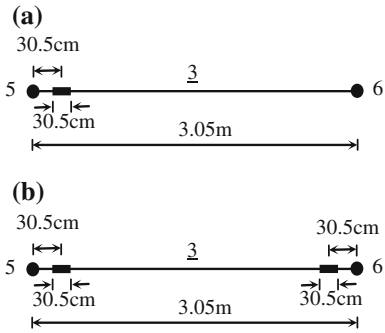

Fig. 5 Defects in the frame

Defect 1

In defect 1, member 3, the beam at the first story level, is considered to have one defect. The cross-sectional area of member 3 is considered to be corroded over a length of 30.5 cm, located at a distance of 30.5 cm from node 5. It is pictorially shown in Fig. 4. The defect is shown in Fig. 5a in the finite element representation.

The web and flange thicknesses are considered to be reduced by 20 % of their original values. The loss of thicknesses will result in the reduction of the cross-sectional area by 19.13 % and the moment of inertia by 17.02 % from the defect-free case. The identified stiffness parameters for all nine members using the GILS-EKF-UI and UKF-UI-WGI methods are summarized in Table 3. In all cases, the maximum changes occur in member 3, indicating it contains the defect. The results also indicate that both methods can be used for RASH of the frame.

Defect 2

In defect case 2, member 3 is considered to have two defects. The first defect is the same as that in defect case 1. For the second defect, the cross-sectional area is also

Table 3 Stiffness parameter (*EI/L*) identification for defect 1

Member	Nominal (N-m)	Change in Identification (%)			
		$R = 10^{-4}$		$R = 10^{-3}$	
		EKF	UKF	EKF	UKF
(1)	(2)	(3)	(4)	(5)	(6)
k_1	96500	−0.008	−0.107	0.048	0.037
k_2	96500	−0.023	0.115	−0.481	−0.314
k_3	96500	**−2.551**	**−2.609**	**−2.371**	**−2.472**
k_4	241250	−0.057	−0.009	−0.015	0.000
k_5	241250	−0.366	−0.148	−0.040	−0.024
k_6	241250	−0.211	−0.158	−0.091	−0.104
k_7	241250	−0.398	−0.099	−0.062	−0.058
k_8	241250	−0.239	−0.402	−0.192	−0.229
k_9	241250	−0.321	−0.411	−0.200	−0.237

Table 4 Stiffness parameter (*EI/L*) identification for defect 2

Member	Nominal (N-m)	Change in Identification (%)			
		$R = 10^{-4}$		$R = 10^{-3}$	
		EKF	UKF	EKF	UKF
(1)	(2)	(3)	(4)	(5)	(6)
k_1	96500	0.131	0.028	0.061	0.022
k_2	96500	−0.347	−0.159	−0.199	−0.141
k_3	96500	**−4.997**	**−5.088**	**−5.189**	**−5.055**
k_4	241250	−0.071	−0.025	−0.091	0.004
k_5	241250	−0.222	−0.020	−0.329	0.016
k_6	241250	−0.223	−0.193	−0.069	−0.055
k_7	241250	−0.467	−0.176	−0.223	−0.192
k_8	241250	−0.440	−0.594	−0.421	−0.653
k_9	241250	−0.508	−0.599	−0.449	−0.661

considered to be corroded over a length of 30.5 cm but it is located at a distance of 30.5 cm from node 6, as shown in Fig. 5b. The identified stiffness parameters for all members using the GILS-EKF-UI and UKF-UI-WGI methods are summarized in Table 4. In all cases, the maximum changes occur in member 3, indicating it contains the defect. The reduction in the stiffness parameter of member 3 for defect 2 is more than that of defect case 1. It is clearly indicated that the defect in case 2 is more severe than that in case 1. The results also indicate that both methods can be used for RASH of the frame.

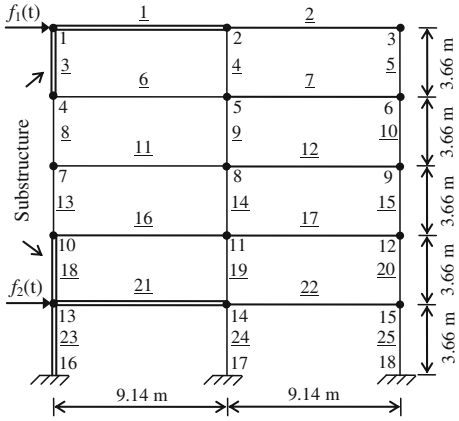

Fig. 6 Finite element representation of a frame

6.2 *Example 2*

In Example 1, both the GILS-EKF-UI and UKF-UI-WGI methods appear to identify the defect spot and the severity accurately. To demonstrate the superiority of UKF-UI-WGI over GILS-EKF-UI, this second example is considered.

6.2.1 Description of the Frame

A two-dimensional frame with a bay width of 9.14 m and story height of 3.66 m, as shown in Fig. 6, is considered. The frame has a total of 25 members; 10 beams and 15 columns. The beams and columns are made of W21 × 68 and W14 × 61 sections, respectively, of Grade 50 steel. The frame is modeled by 18 nodes in the finite element (FE) representation. Each node has three dynamic degrees of freedom (DDOFs); two translational and one rotational. The support condition at the base (nodes 16, 17, and 18) of the frame is considered to be fixed. The total number of DDOFs for the frame is 45. The actual theoretical stiffness parameter values k_i evaluated in terms of (E_iI_i/L_i) are calculated to be 13476 kN-m and 14553 kN-m for a typical beam and column, respectively. First two natural frequencies of the frame are estimated to be f_1 = 3.598 Hz and f_2 = 11.231 Hz, respectively. Following the procedure described in [6], Rayleigh damping coefficient α and β are calculated to be 1.7122088 and 0.00107326, respectively, for an equivalent modal damping of 5 % (commonly used in model codes in the US) of the critical for the first two modes.

The frame is excited simultaneously by two sinusoidal loadings. The first loading, $f_1(t)$ = 3 sin(18t) kN is applied horizontally at node 1, and the second loading, $f_2(t)$ = 2 sin(22t) kN is applied horizontally at node 13, as shown in Fig. 6. For this example, the information on responses are numerically generated using a commercially available software ANSYS (ver. 15.0) [5]. The responses are

obtained at 0.0001 s time interval. After the responses are simulated, the information on input excitations is completely ignored. Responses between 0.02 and 0.32 s providing 3001 time points are used in the subsequent health assessment process.

6.2.2 Identification of the State of the Frame

Two substructures are considered to assess the health of this large frame. They are shown in Fig. 6 with double lines. Using responses at 18 DDOFs in the substructures, the stiffness and damping parameters and the time history of unknown input force are identified using the ILS-UI procedure in Stage 1, initially for the defect-free state of the frame. The errors in identification of the stiffness parameters are shown in Table 5. From the results, it can be observed that the errors in the identified stiffness parameter of the five members in the substructures are very small. The damping coefficients and excitation time history are also identified very accurately.

The information of Stage 1 is used to initiate both the GILS-EKF-UI and UKF-UI-WGI procedures. Then, the stiffness parameters of all 25 elements of the frame are estimated. The stiffness parameters of all members in the frame are identified for the defect-free state and the results are summarized in Table 6, Columns 3 and 4, respectively, for both methods. Since the identified stiffness parameter did not vary significantly from the expected values, the methods correctly identified the defect-free state of the frame. The results of GILS-EKF-UI are still within the acceptable level but not as good as the UKF-UI-WGI method. However, it can be concluded that both filters identified the defect-free state of the frame.

After assessing structural health of the defect-free frame, one defective case is considered for this example. In Defect 1, the cross-sectional area of member 17 is considered to be corroded over a length of 30 cm, located at a distance of 30 cm from node 12. The results for the substructure identification in Stage 1 using ILS-UI are summarized in Table 5, Columns 5 and 6. As for the defect-free case, for this defective state, the substructures are identified accurately. Using the information from Stage 1, the whole frame is then identified using both methods in Stage 2. The

Table 5 Stiffness parameter (*EI/L*) identification of the substructure for Example 2

Member	Theoretical (kN-m)	Defect Free		Defect 1	
		Identified	Change (%)	Identified	Change (%)
(1)	(2)	(3)	(4)	(5)	(6)
k_1	13476	13476	0.001	13476	0.001
k_3	14553	14553	0.001	14553	0.001
k_{18}	14553	14553	0.004	14553	0.003
k_{21}	13476	13477	0.003	13477	0.003
k_{23}	14553	14553	0.004	14553	0.003

Table 6 Change (%) in stiffness parameter (*EI/L*) identification of whole structure

Member	Theoretical (kN-m)	Defect Free		Defect 1	
		EKF	UKF	EKF	UKF
(1)	(2)	(3)	(4)	(5)	(6)
k_1	13476	−0.05	−0.07	−0.07	−0.06
k_2	13476	−0.37	0.37	−6.84	0.87
k_3	14553	−0.03	−0.05	−0.07	−0.05
k_4	14553	0.03	0.17	−1.96	0.20
k_5	14553	0.76	−0.13	11.23	−1.00
k_6	13476	−0.06	−0.02	0.73	−0.02
k_7	13476	−0.04	−0.21	1.90	0.06
k_8	14553	0.41	0.67	−0.12	0.62
k_9	14553	0.38	0.57	−2.88	0.37
k_{10}	14553	0.69	0.22	7.31	1.37
k_{11}	13476	0.51	0.09	2.43	0.25
k_{12}	13476	−0.25	0.01	−2.06	−0.71
k_{13}	14553	−0.68	−0.55	−1.07	−0.57
k_{14}	14553	−1.57	−0.81	−4.68	−1.69
k_{15}	14553	0.07	−1.17	4.42	−0.13
k_{16}	13476	0.40	0.26	0.56	−0.09
k_{17}	13476	1.24	1.01	**−7.54**	**−8.39**
k_{18}	14553	0.01	0.02	0.17	0.05
k_{19}	14553	−0.69	−0.45	−1.07	−0.42
k_{20}	14553	0.26	0.02	−1.25	−1.16
k_{21}	13476	0.07	0.04	0.18	0.05
k_{22}	13476	−0.52	−0.45	−1.34	−0.97
k_{23}	14553	0.14	0.06	0.18	0.05
k_{24}	14553	0.09	0.00	0.02	0.05
k_{25}	14553	0.15	0.34	0.67	0.62

results in Columns 5 and 6 in Table 6 clearly indicate that the UKF-UI-WGI procedure is capable of identifying the location and severity of defect. The identification of defect location using the GILS-EKF-UI procedure for the defective case is not straightforward. Both the UKF and EKF-based procedures identified the reductions of the stiffness parameter of defective member 17 as 8.39 and 7.54 %, respectively. However, the results of EKF-based procedure show that the stiffness parameter of defect-free member 5 is increased by 11.23 %, which is more than acceptable error. Therefore, it can be concluded that GILS-EKF-UI failed to assess the health of the frame for the defective state. This example clearly demonstrates the superiority of the proposed UKF-UI-WGI procedure over the GILS-EKF-UI procedure developed earlier by the research team.

7 Conclusions

The rapid assessment of structural health has become a major challenge in the context of routine maintenance or just after major natural and man-made events. The authors and their team members used the system-identification techniques by mitigating its weaknesses to identify defects and their severity at the local element level by representing real structures using finite elements. For easier implementation, the excitation information was completely ignored. By tracking the changes in the stiffness parameters of each element the location(s) and severity of defects are assessed. The team conducted extensive analytical and laboratory investigations to verify all the methods. They had to overcome several challenges related to the conceptual and analytical development, data processing, and the presence of uncertainty in the every phase. To consider nonlinearity in the system identification process, a method known as Generalized Iterative Least Squares-Extended Kalman Filter-Unknown Input (GILS-EKF-UI), was developed by the team earlier. Since it failed to identify structures in some cases, the authors recently proposed a new method denoted as Unscented Kalman Filter—Unknown Input- Weighted Global Iterations (UKF-UI-WGI). With the help of informative examples, the superiority of UKF-UI-WGI over GILS-EKF-UI is documented in this paper. Since at the beginning of an inspection, the defects and their severity are expected to be unknown, the authors recommend UKF-UI-WGI instead of GILS-EKF-UI for the rapid assessment of health of infrastructures.

Acknowledgments The authors would like to thank all the team members for their help in developing the overall research concept of structural health assessment and monitoring. They include Drs. Duan Wang, Peter H. Vo, Xiaolin Ling, Hasan N. Katkhuda, Rene Martinez-Flores, Ajoy K. Das, Mr. J. P. Kazakoff and A. R. Safdar. The team received financial supports from the National Science Foundation, a small grant from the University of Arizona, graduate student supports from various sources including Raytheon Missile Corporation, Ministry of Higher Education, Jordon, CONACYT, Iraq's Ministry of Higher Education and Scientific Research, Department of Civil Engineering and Engineering Mechanics, University of Arizona, etc. The financial supports from the National Science Foundation; most recently under Grant No. CMMI-1403844 is also appreciated. Any opinions, findings, or recommendations expressed in this paper are those of the writers and do not necessarily reflect the views of the sponsors.

References

1. Al-Hussein A, Haldar A (2015) A comparison of unscented and extended Kalman filtering for nonlinear system identification. In: 12th international conference on applications of statistics and probability in civil engineering (ICASP12-2015). Vancouver, Canada
2. Al-Hussein A, Haldar A (2015) Novel unscented Kalman filter for health assessment of structural systems with unknown input. J Eng Mech ASCE 141(7):04015012-1–04015012-13. doi:10.1061/(ASCE)EM.1943-7889.0000926
3. Al-Hussein A, Haldar A (2015) Structural health assessment at a local level using minimum information. Eng Struct 88:100–110. doi:10.1016/j.engstruct.2015.01.026

4. Al-Hussein A, Haldar A (2015) Unscented Kalman filter with unknown input and weighted global iteration for health assessment of large structural systems. Structural Control and Health Monitoring. doi:10.1002/stc.1764
5. ANSYS version 15.0 (2013).The Engineering Solutions Company
6. Clough RW, Penzien J (2003) Dynamics of structures, 3rd edn. Computers and Structures, California
7. Cross EJ, Worden K, Farrar CR (2013) Chapter 1—structural health assessment for civil infrastructure. Health Assessment of Engineered Structures: Bridges, Buildings and Other Infrastructures, World Scientific Publishing Co., Editor, pp 1–31
8. Das AK (2012) Health assessment of three dimensional large structural systems using limited uncertain dynamic response information. PhD dissertation, Department of Civil Engineering and Engineering Mechanics, University of Arizona, Tucson, Arizona
9. Haldar A (ed) (2013) Health assessment of engineered structures: bridges, buildings and other infrastructures. World Scientific Publishing Co., New Jersey
10. Haldar A, Das AK, Al-Hussein A (2013) Data analysis challenges in structural health assessment using measured dynamic responses. Adv Adapt Data Anal 5(4):1350017-1–1350017-22
11. Hoshiya M, Saito E (1984) Structural identification by extended Kalman filter. J Eng Mech ASCE 110(12):1757–1772
12. Jazwinski AH (1970) Stochastic process and filtering theory. Academic Press, Inc., New York
13. Julier SJ, Uhlmann JK (2004) Unscented filtering and nonlinear estimation. In: Proceedings of the IEEE, vol 92, no 3, pp 401–422
14. Julier SJ, Uhlmann JK, Durrant-Whyte HF (1995) A new approach for filtering nonlinear systems. In: Proceedings of the american control conference, vol 3. Seattle, Washington, pp 1628–1632
15. Kalman RE (1960) A new approach to linear filtering and prediction problems. Trans ASME J Basic Eng 82:35–45
16. Kalman RE, Bucy RS (1961) New results in linear filtering and prediction theory. J Fluids Eng 83(1):95–108
17. Katkhuda H, Haldar A (2008) A novel health assessment technique with minimum information. Struct Control Health Monit 15(6):821–838
18. Katkhuda H, Martinez-Flores R, Haldar A (2005) Health assessment at local level with unknown input excitation. J Struct Eng ASCE 131(6):956–965
19. Ling X, Haldar A (2004) Element level system identification with unknown input with Rayleigh damping. J Eng Mech ASCE 130(8):877–885
20. Martinez-Flores R (2005) Damage assessment potential of a novel system identification technique—experimental verification. PhD dissertation, Department of Civil Engineering and Engineering Mechanics, University of Arizona, Tucson, Arizona
21. Maybeck PS (1979) Stochastic models, estimation, and control theory. Academic Press Inc, UK
22. Vo PH, Haldar A (2003) Post-processing of linear accelerometer data in structural identification. J Struct Eng 30(2):123–130
23. Vo PH, Haldar A (2008) Health assessment of beams—experimental verification. Struct Infrastruct Eng 4(1):45–56
24. Wang D, Haldar A (1994) Element-level system identification with unknown input information. J Eng Mech ASCE 120(1):159–176
25. Wang D, Haldar A (1997) System identification with limited observations and without input. J Eng Mech ASCE 123(5):504–511
26. Welch G, Bishop G (1995) An introduction to the Kalman filter. Technical report TR95-041, Department of Computer Science, University of North Carolina at Chapel Hill, Chapel Hill, NC, USA